Dynamics of network oscillations: power grid stability analysis applications

Andrey Churkin
Center for Energy Science and Technology
Skolkovo Institute of Science and Technology (Skoltech)
Moscow, Russia
andrey.churkin@skolkovotech.ru

Abstract

Studies on the synchronization of oscillators found numerous practical applications. Analysis of power system stability is an essential one: power generators rotate at angular frequencies and influence each other via power lines, thus, forming a network of oscillators. Recently a prominent concept of basin stability was developed to measure the ability of generators to withstand large perturbations without losing the synchronization. In this paper, we analyze the numerical issues that arise in power system dynamics simulation and their effect on the basin stability estimations. Specifically, we used explicit Runge-Kutta methods for composing the stability basin of a one-node system and performed a convergence analysis. We found that the accuracy and time step of the methods may significantly influence the estimation of the system's stability. Analysis of the errors shows that it is preferable to use higher order Runge-Kutta methods to reach a better balance between accuracy and computational cost.

1 Introduction

Synchronization of oscillators is a widely known phenomenon that takes place in a variety of natural and engineering systems. Usually, oscillators influence each other in a certain order and with a strength that depends on physical assumptions and topology of the model. Therefore, such systems are often referred to as networks

of oscillators. Initially, the basic aim of oscillators dynamics analysis was to estimate the convergence of a system to a desired synchronous state. Numerous mathematical models have been developed to describe synchronization in oscillator networks. One of the notable ones, the Kuramoto model [1], formulates the interactions as a sinusoidal dependence on the phase difference between each pair of oscillators:

$$\dot{\theta}_i = \omega_i + \frac{K}{N}\sum_{j=1}^{N} \sin(\theta_j - \theta_i), \qquad i = 1 \dots N \tag{1}$$

,where ω_i is the natural frequency of oscillator i, and K is the coupling strength.

Later, more sophisticated models of oscillator networks were developed that allowed analysis of complex dynamics with exotic states of synchronization. *Matheny et al.* [2] examined exotic states (weak chimeras, decoupled states, traveling waves, inhomogeneous synchronized states) in a network of nanoelectromechanical oscillators. The authors used a high-order model that comprised a ring of coupled quasi-sinusoidal oscillators and demonstrated the dynamical richness of complex systems. Chimera states were thoroughly studied by *Abrams and Strogatz* [3], who derived an exact chimera state solution for a ring of coupled oscillators. Recently, *Nicolaou et al.* [4] introduced the Janus oscillator model that contains a network with pairs of nonidentical phase oscillators. It was shown that such networks exhibit numerous dynamic phenomena such as explosive synchronization, traveling, intermittent, and bouncing chimeras.

One of the practical applications of the synchronization models was found in power system stability analysis. The analogy lies in the fact that power generators rotate at angular frequencies and influence each other via power lines, thus, forming a network of oscillators. *Filatrella et al.* [5] implemented the Kuramoto model for a power grid. The dynamics of generators was simulated to estimate the stability of the system against perturbations. The comparative analysis of existing models for power-grid synchronization was done by *Nishikawa and Motter* [6]. Such models are widely used for modeling transient regimes of power systems and analyzing dynamic stability. In [7], *Schäfer et al.* used a power system dynamic model to simulate cascading failures and proposed a forecasting method for critical lines identification. In this paper, we focus on the stability analysis concept proposed by *Menck et al.* [8] that is based on determining power grid responses to large perturbations and composing the basin of attraction of the synchronous state. Menck demonstrated how stability basins could be evaluated for each node of a power system and introduced a stability index that is the ratio of the basin's volume to the considered space of possible regimes. This concept allows analyzing the grid's degree of stability

against large single-node perturbations and suggests ways of improving network topology.

Menck's study resonated with the research community and led to a series of subsequent works. Kim et al. [9] investigated the functional form of the basin stability's dependence on transmission strength. The authors analyzed several small networks with different topologies and classified basin stability transition patterns. *Mitra et al.* [10] extended the concept of basin stability for a multi-node framework. The method considers multiple simultaneous perturbations and enables estimation of the minimum number of nodes of the network to be controlled or protected from external perturbations to ensure proper operation of the system. Liu et al. [11] incorporated a sixth-order generator model and used the basin stability concept to rank the transient stability of generators in power systems.

In this paper, we use the basin stability concept to analyze numerical issues that arise in power system dynamics simulation. We compose the stability basin for a one-node system using explicit iterative methods with different time steps and perform a convergence analysis.

2 Model description

To examine the behavior of network oscillations in power systems, we simulate local power imbalances and consequent electromechanical dynamics. We consider the classical dynamic power grid model widely known as the swing equation [12]:

$$\dot{\theta}_i = \omega_i \tag{2}$$

$$M_i \omega_s \dot{\omega}_\iota = -D_i \omega_i + L_i^{in} - G_{ii} V_i^2 - \sum_{j=1}^{N} Y_{ij} V_i V_j \sin(\theta_i - \theta_j) \tag{3}$$

where θ_i, ω_i, and V_i represent the phase angle, angular frequency and voltage magnitude at generator i. The synchronous state corresponds to a regime where angular frequency equals the rated grid's frequency ω_s. M_i stands for the cumulative moment of inertia of the masses represented by node i (angular momentum of rotor). L_i^{in} is the power injection, and $G_{ii}V_i^2$ is the amount of power consumed or injected by loads and renewable generation devices (both terms can be aggregated to the net injected power L_i). D_i is the damping coefficient. Y_{ij} is the admittance matrix that equals $1/X_{ij}$, where X_{ij} stands for the reactance of a transmission line between nodes i and j. Thus, the model (2)-(3) incorporates frequency dynamics based on the balance of active power. It describes the electromechanical synchronization of coupled oscillators (generators) and corresponds to a second-order Kuramoto model [1].

We consider a one-node system where a single generator connected to an external power system supplies local demand via a transmission line. For a single-generator system, the model (2)-(3) can be modified by dividing equation (3) by $M_i\omega_s$:

$$\dot{\theta} = \omega \tag{4}$$

$$\dot{\omega} = -\alpha\omega + P - K\sin(\theta - \theta_{grid}) \tag{5}$$

where $\alpha = D/M\omega_s$ represents the damping effect, $P = L_i/M\omega_s$ is the net power input (generation minus consumption), and $K = Y_{ij}V_iV_j/M\omega_s$ stands for the capacity of the power line. The phase angle of an external grid θ_{grid} is considered equal zero.

A stable synchronous regime implies that $\omega = 0$ (in a reference frame of the grid's rated frequency). In case of loss of synchronization, the generation will accelerate, and its angular frequency will reach the non-synchronous limit cycle. As shown in [8] , the cycle can be evaluated as a function of time:

$$\omega_{ns} \approx \frac{P}{\alpha} + \frac{\alpha K}{P}\cos\left(\frac{P}{\alpha}t\right) \tag{6}$$

In the following sections, we analyze the dynamics of the one-node model synchronization depending on the initial conditions.

3 Basin stability analysis

We follow the analysis presented in [8] and consider a one-node model with damping factor α=0.1, net power input P=1, and transmission capacity K=8. The model (4)-(5) is the initial value problem for the system of time-dependent ordinary differential equations. Thus, the outcome after time t depends on the initial regime (θ_0 and ω_0). The deviation in the initial regime from the synchronous state can be caused by sudden changes in load, short circuits, or other circumstances that force the generator to accelerate or slow down. We visualize the possible outcomes in Figures 1 and 2. In both cases, the generator got slowed down before the synchronization process and had negative angular frequency. In the first case ($\theta_0 = 3$, $\omega_0 = -5$), the generator accelerated enough to reach the synchronous state ($\omega = 0$). However, the slightly different initial regime ($\theta_0 = 3$, $\omega_0 = -6$) led to the loss of synchronization: the angular frequency did not settle to zero, and the phase angle continued growing infinitely.

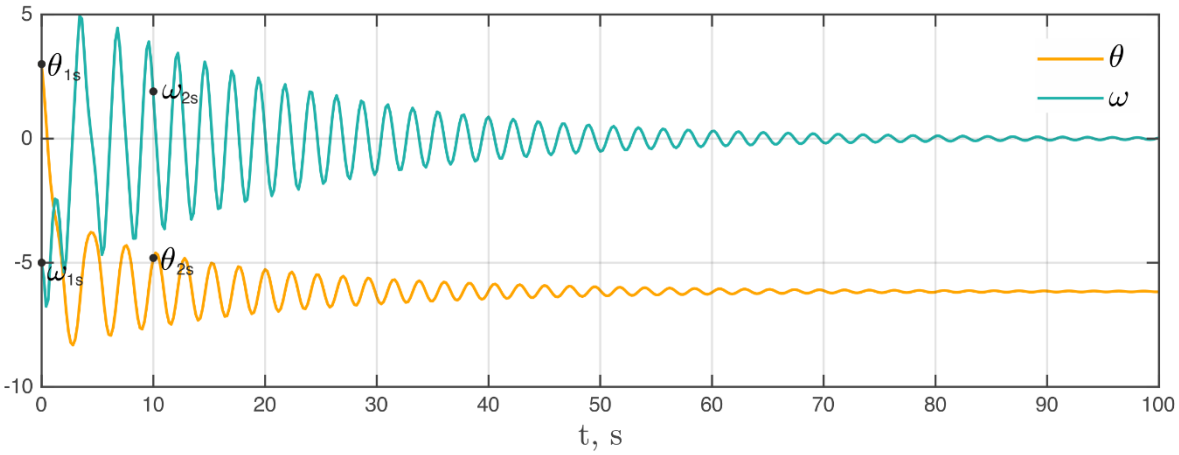

Figure 1: Synchronization after initial regime $\theta_0 = 3$, $\omega_0 = -5$.

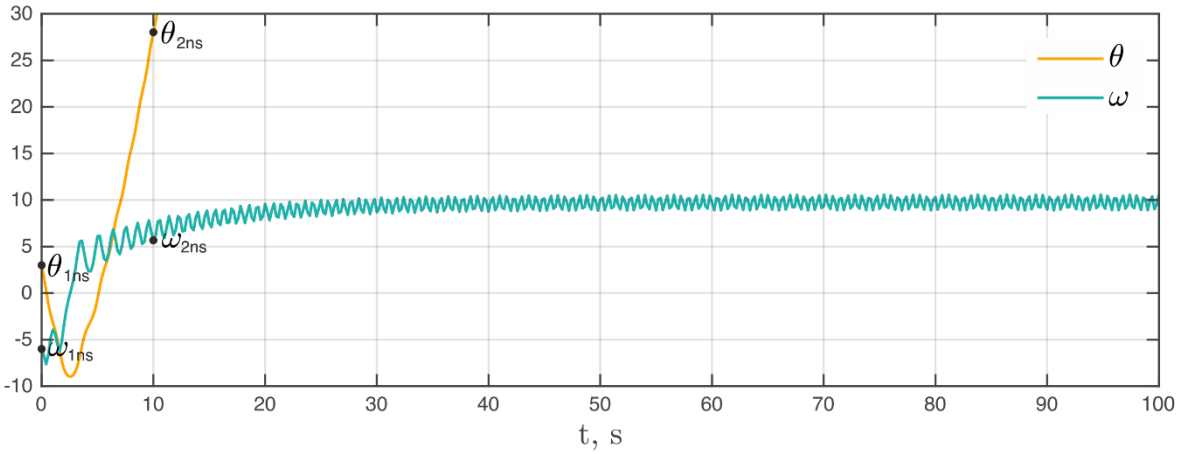

Figure 2: Loss of synchronization after initial regime $\theta_0 = 3$, $\omega_0 = -6$.

We used the fourth order explicit Runge–Kutta method (RK4) for solving system (4)-(5) with a time step h=0.2 s. To check the convergence of the algorithm, we solved the system one more time with a more accurate time step h=0.05 s. The error was estimated as the difference between the coarse and the accurate solutions. Figure 3 shows that the differences in the solutions decrease with time. The algorithm with a coarse time step underestimated the oscillations. Thus, the synchronous state was reached faster with h=0.2. An intermediate conclusion can be drawn that the algorithm converges for problems with initial conditions leading to synchronization. However, as shown in the following discussions, this may not always be the case.

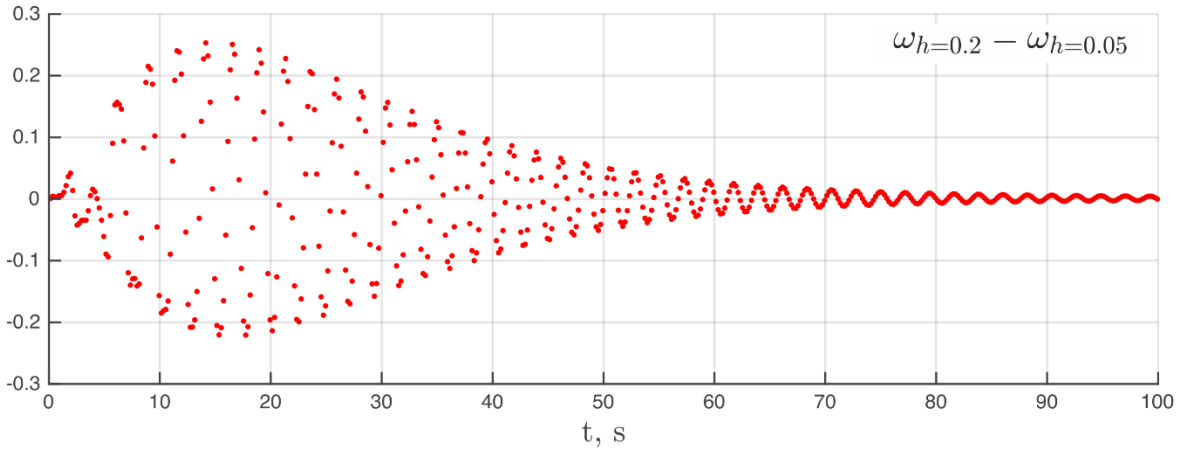

Figure 3: Error estimation of the RK4 method applied to the system (4)-(5) with a synchronization after initial regime and time steps h=0.2, h=0.05 s.

To analyze basin stability of the generator in the one-node model, we solve the system (4)-(5) for 40.401 regimes, varying initial values in the range $\theta_0 = [-\pi : \pi]$, $\omega_0 = [-15 : 15]$. The outcomes were recognized as synchronization if the angular frequency settled to the range [-1:1] after the first 60 seconds of simulations. The corresponding initial conditions were highlighted green in Figure 4. The regimes leading to a loss of synchronization were highlighted red. The red line at the top of the figure represents the non-synchronous limit cycle (6).

The regimes simulated in Figures 1 and 2 are also depicted in the stability basin. For convenience, we plot only the first 10 seconds of the oscillations. The regime "1s" leads to a synchronous state where the solution reaches the major green region and starts swinging towards its center. The "1ns" initial values make the generator accelerating up to point "2ns" and further up to the non-synchronous limit cycle. According to [8], the basin stability can be measured as the likelihood that the system returns to the synchronous state after having been hit by a large perturbation. Thus, we estimate the stability index as the ratio of the green points to all possible initial conditions in the considered range. For the case with transmission capacity K=8, the stability index S=0.3879 based on the analysis of 40.401 points.

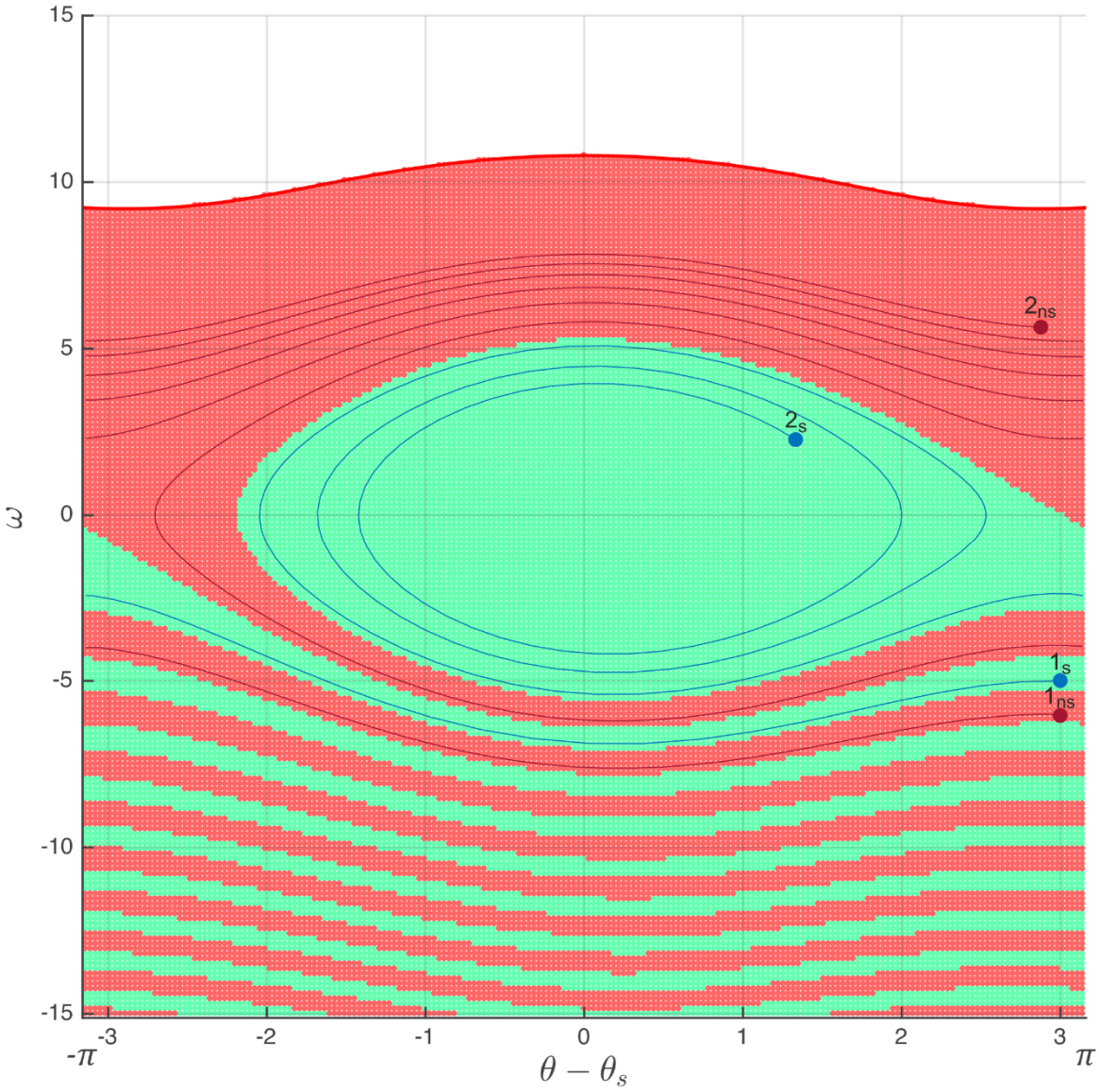

Figure 4: Basin stability for K=8, evaluated with a time step h=0.2.

We repeat the simulation for the increased transmission capacity K=16 and plot the stability basin in Figure 5. It is seen that the green regions enlarged significantly. The new stability index reached S=0.543.

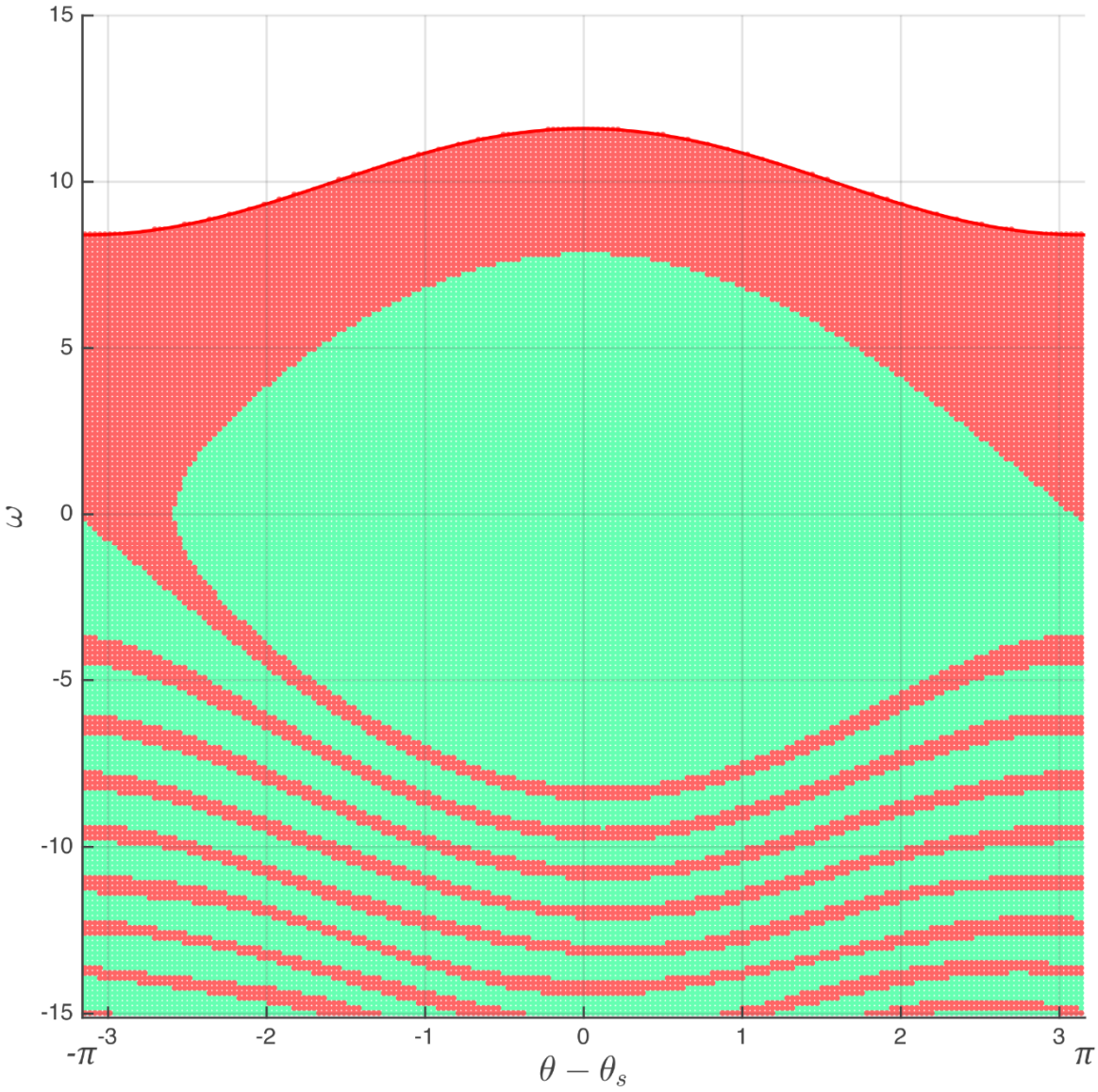

Figure 5: Basin stability for K=16, evaluated with a time step h=0.2.

4 Convergence of the explicit multistage methods

To further analyze the convergence of the explicit multistage method for the dynamic power grid model (4)-(5), we estimate the same stability basin as in Figure 4 but with a coarse time step h=0.4. The modified basin is shown in Figure 6. We see that the regions got significantly deformed, especially at the bottom of the figure. The modified stability index changed to S=0.4166. Indeed, the method with a coarse time step underestimated some oscillations and mistakenly enlarged the stability region.

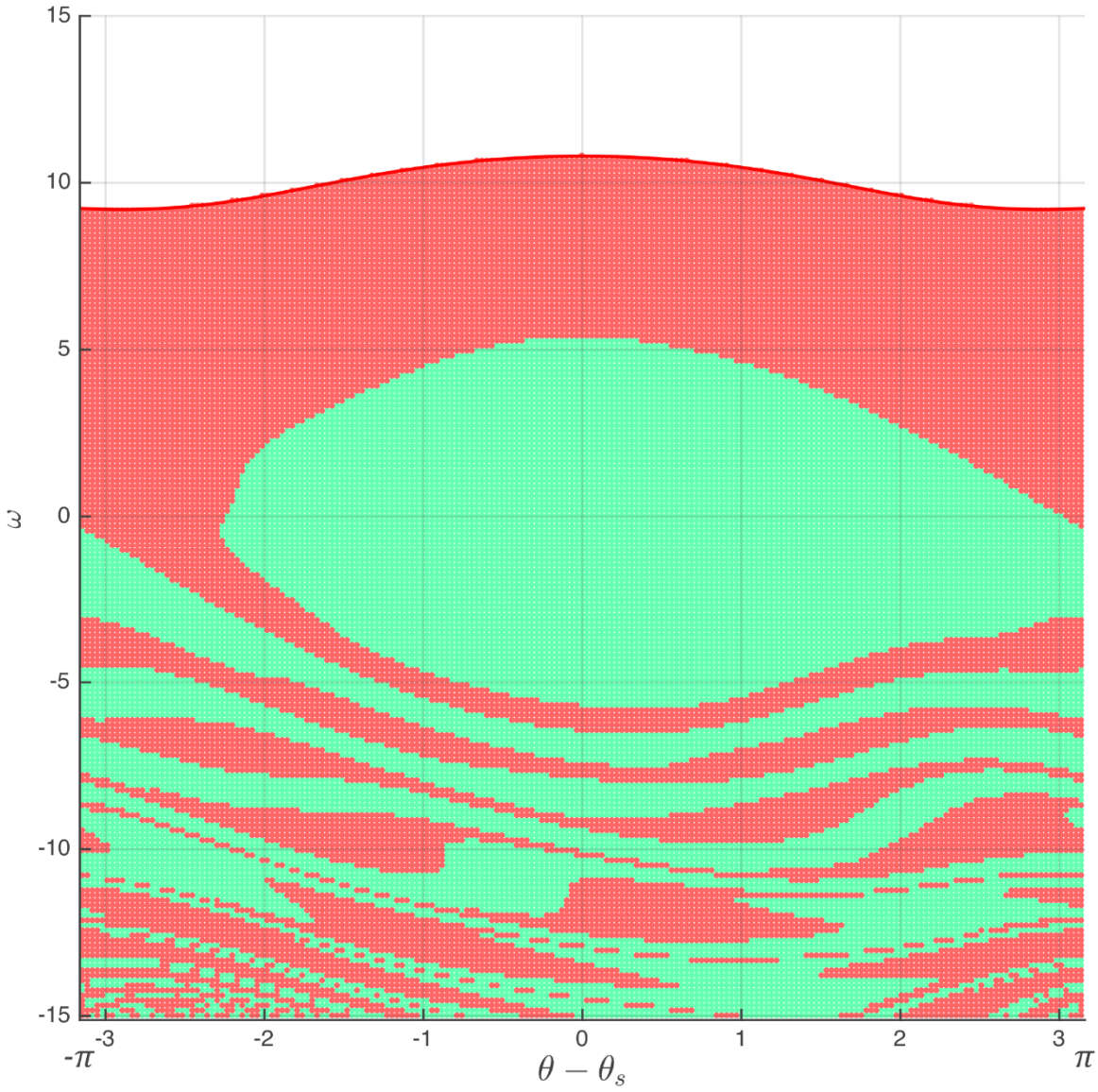

Figure 6: Basin stability for K=8, evaluated with a time step h=0.4.

We present the comparison of the stability basins obtained by the methods with time steps h=0.2 and h=0.4 s in Figure 7. If the accurate and the coarse solutions agree, we keep the colors for such points (green for synchronization cases, red for loss of synchrony). The red-filled dots with green borders depict the initial values for which the accurate algorithm with h=0.2 identifies the loss of synchrony, and the algorithm with h=0.4 does not. The opposite cases (the accurate algorithm with h=0.2 predicts the synchronization, and the algorithm with h=0.4 identifies the loss of synchrony) are represented by green-filled dots with red borders.

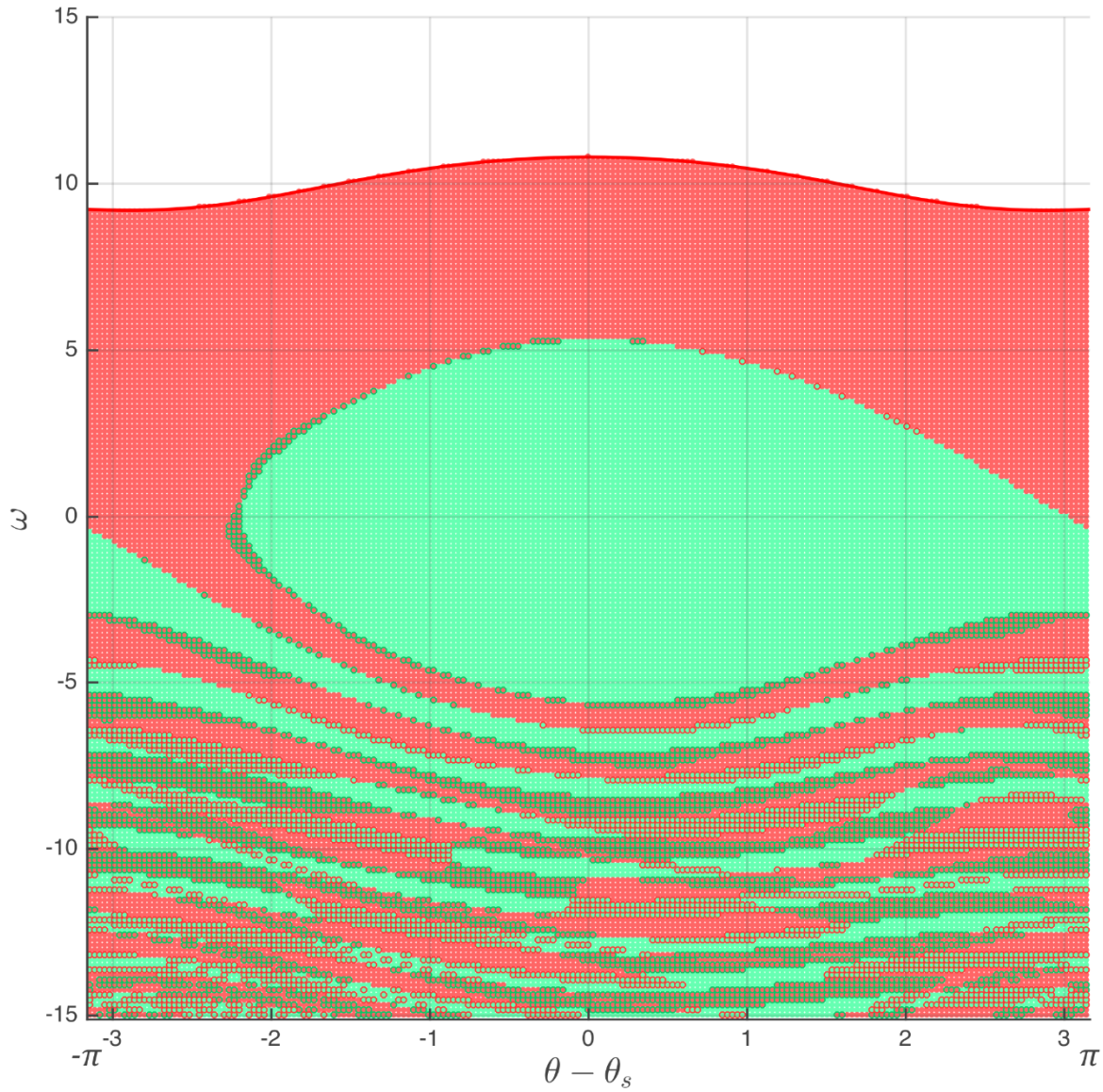

Figure 7: Comparison of the solutions for K=8 by the methods with time steps h=0.2 and h=0.4 s.

It is worth mentioning that we found both cases happening for the same stability basin. Some initial values led the algorithm with a coarse time step to overestimate the oscillations, while others - to overlook cases of synchrony loss. In our particular example, the cases of oscillation smoothing prevailed (red-filled dots with green borders). Therefore, the modified stability index was mistakenly increased.

We selected two cases for which the outcomes of the algorithms diverge and illustrated them in Figures 8 and 9. In Figure 8, we see that the dynamic process simulated by the algorithm with h=0.4 smoothed the initial oscillations. Then, the angular frequency started settling down to the synchronous state. On the contrary,

the simulations in Figure 9 show that for some values, the algorithm with h=0.4 overestimated the oscillations and erroneously identified the synchrony loss.

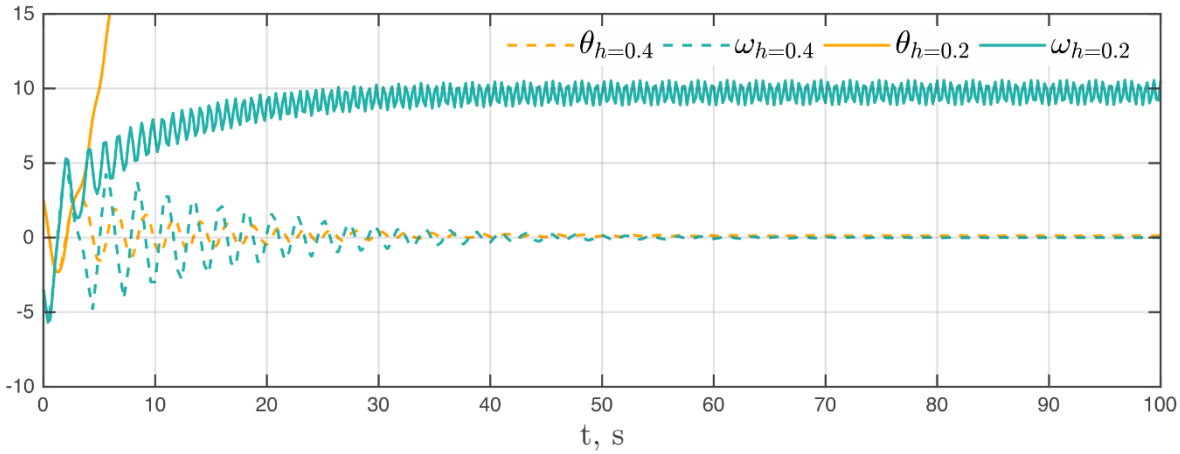

Figure 8: Divergence in the solutions by the algorithms with time steps h=0.2 and h=0.4 s for the initial conditions $\theta_0 = 2.5$, $\omega_0 = -3.5$.

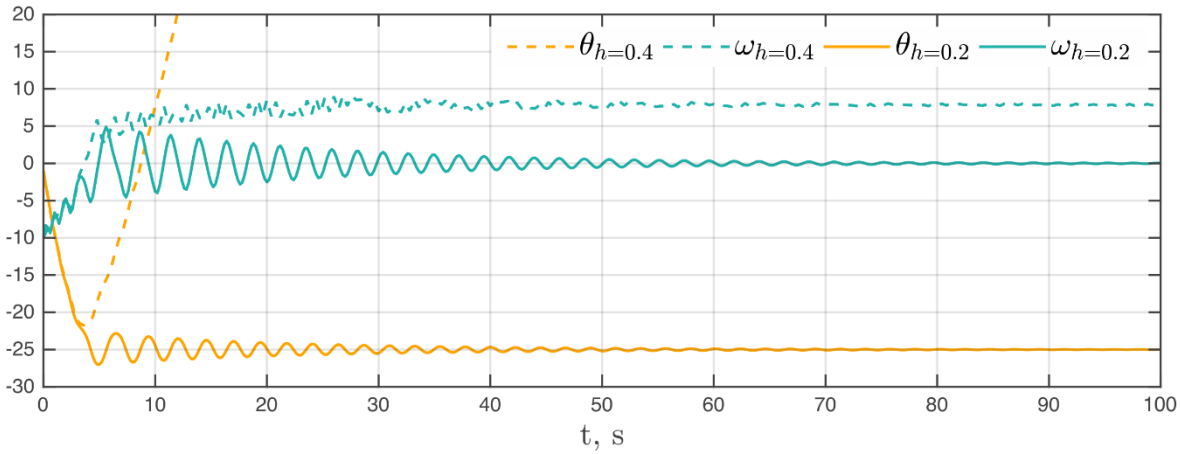

Figure 9: Divergence in the solutions by the algorithms with time steps h=0.2 and h=0.4 s for the initial conditions $\theta_0 = -1$, $\omega_0 = -10$.

The above simulations show that basin stability analysis highly depends on the accuracy and time step of an iterative algorithm. Depending on the initial conditions, it is both possible to underestimate or overestimate the stability of a system. To identify appropriate time steps for our model, we launched a series of simulations for the two selected cases (depicted in Figures 8 and 9) using second order and fourth order Runge-Kutta methods (RK2 and RK4). The solution obtained by RK4 with the time step $h=10^{-4}$ was considered as the accurate one to estimate the errors of other solutions. The norms of the errors are presented in Figures 10 and 11.

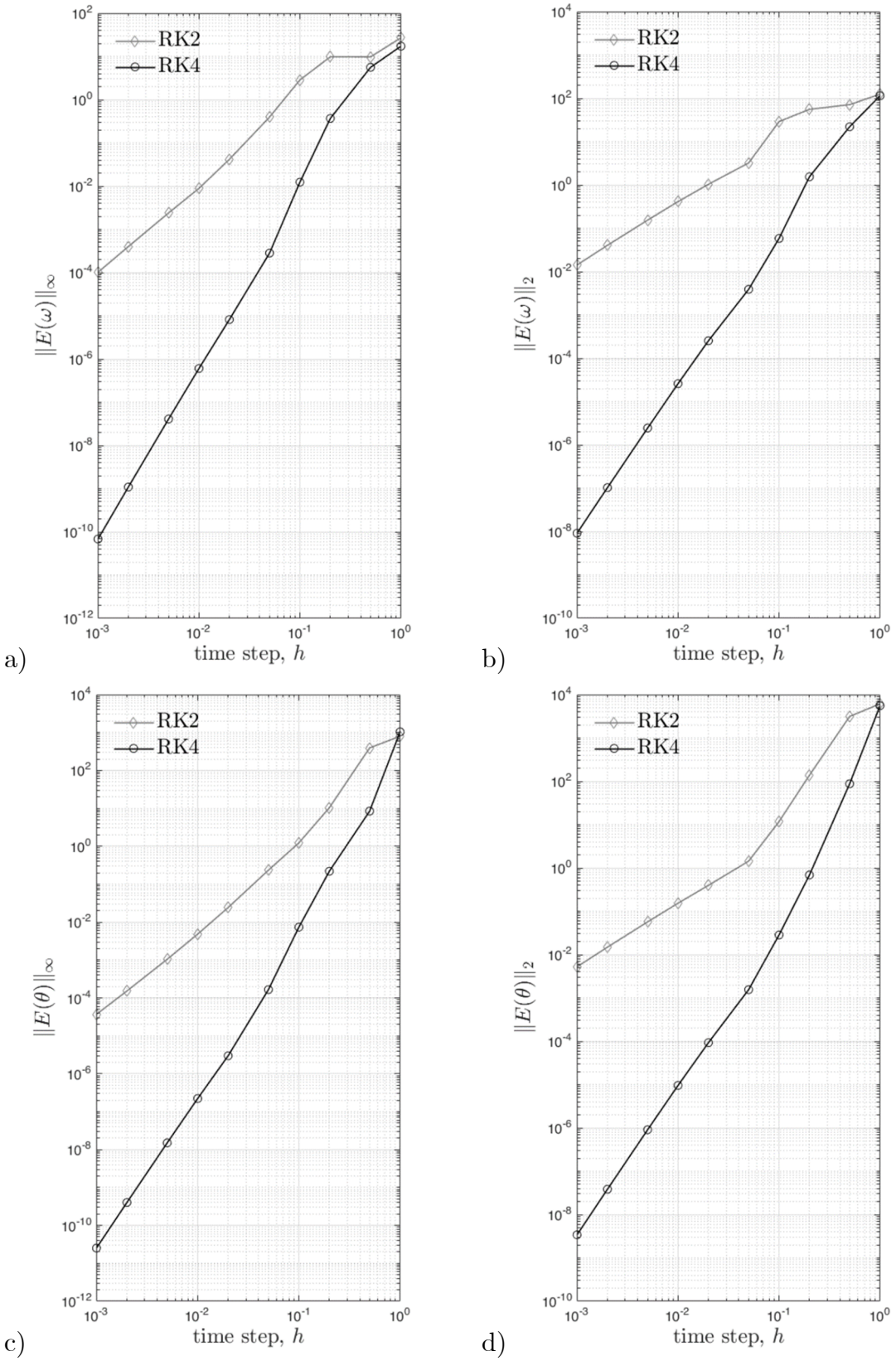

Figure 10: Error estimation of the RK2 and RK4 methods with time steps in $[10^{-3}:1]$ and initial regime $\theta_0 = -1$, $\omega_0 = -10$.

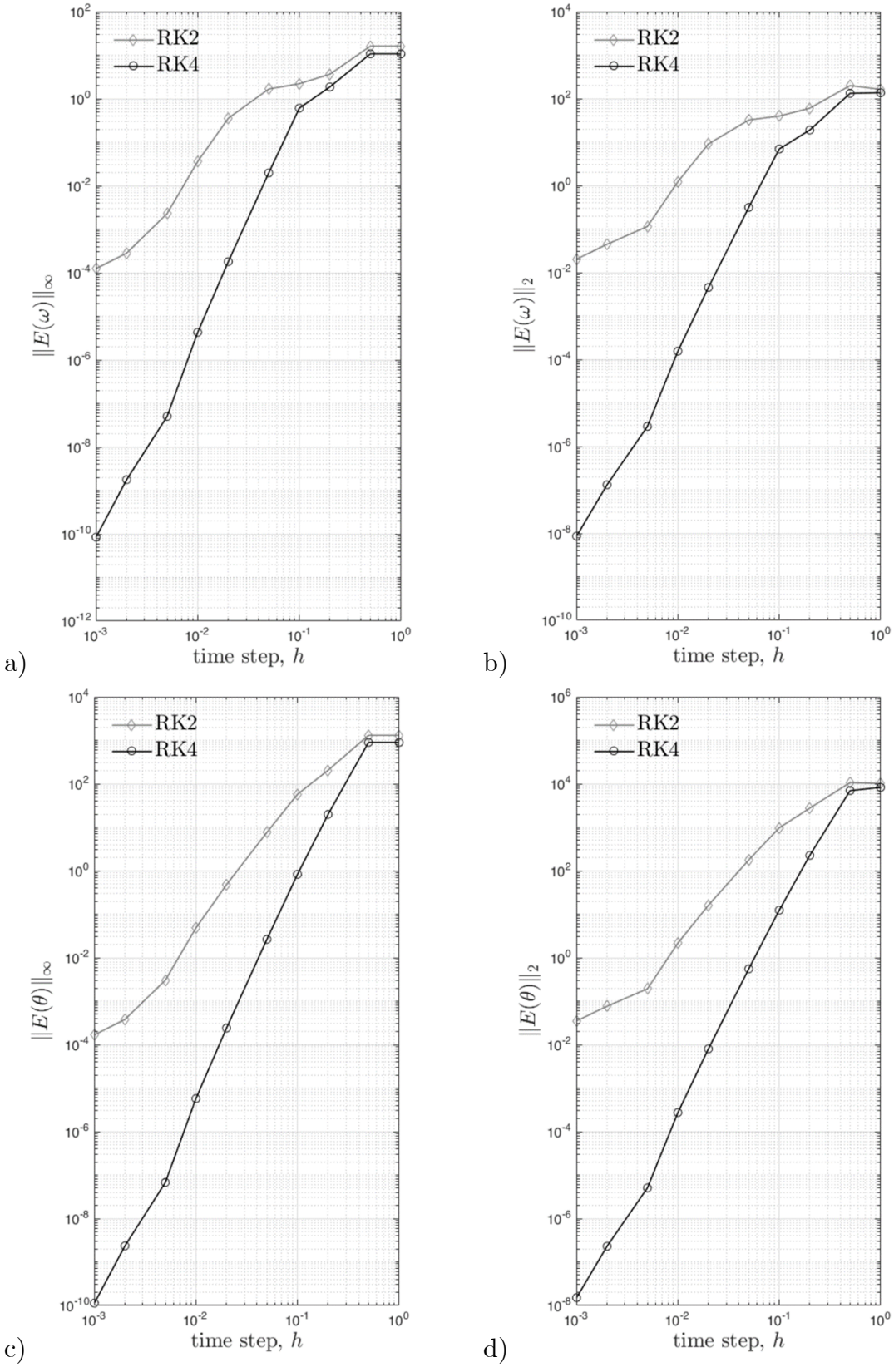

Figure 11: Error estimation of the RK2 and RK4 methods with time steps in $[10^{-3}{:}1]$ and initial regime $\theta_0 = 2.5$, $\omega_0 = -3.5$.

It is seen that RK4 achieves the fourth order accuracy for our problem while RK2 highly depends on the time interval and sometimes does not allow to obtain reasonable accuracy. Our first observation is that errors in phase angles increase faster and reach higher values than errors in angular frequencies. This happens because low-accuracy algorithms identify different states (synchronous state or loss of synchronization) compared to the accurate solutions. Thus, the phase angles of the generator deviate a lot in such solutions. We should also notice that even though the algorithms reach similar accuracy in Figures 10 and 11, the trajectories of the errors differ significantly. In case when the accurate solution leads to an asynchronous state (Figure 10), the errors of the algorithms straightly decrease along with the time step. However, in case of the loss of synchrony (Figure 11), error trajectories are not smooth. It takes smaller time steps to reach equivalent accuracy for such initial conditions.

The computational costs of RK2 and RK4 for different time steps are given in Figure 12. The RK4 method requires about twice as much time as RK2 to obtain a solution with the same time step. However, as shown in Figures 10 and 11, there could be a difference of several orders in the accuracies. Therefore, it should be recommended to use RK4 as the superior method in terms of accuracy/cost balance.

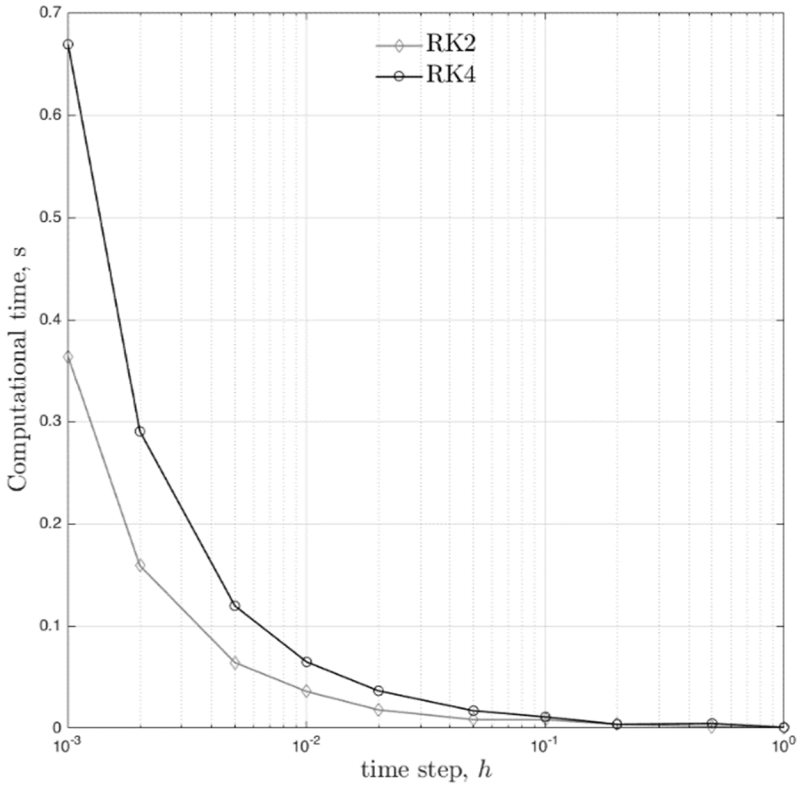

Figure 12: The computational cost of the RK2 and RK4 methods.

5 Conclusions

In this work, we studied numerical aspects of modeling oscillations in power systems. Namely, we applied the basin stability concept to a one-node system and analyzed its stability against large perturbations. Explicit Runge-Kutta methods were used to solve the initial value problem posed by the classical swing equation system. We found that the accuracy and the time step of the methods may significantly influence the estimation of the system's stability. Analysis of the errors shows that it is preferable to use higher order Runge-Kutta methods to reach a better balance between accuracy and computational cost.

References

[1] Y. Kuramoto, "International Symposium on Mathematical Problems in Theoretical Physics," 1975.

[2] M. H. Matheny *et al.*, "Exotic states in a simple network of nanoelectromechanical oscillators," *Science (80-.).*, 2019.

[3] D. M. Abrams and S. H. Strogatz, "Chimera states for coupled oscillators," *Phys. Rev. Lett.*, 2004.

[4] Z. G. Nicolaou, D. Eroglu, and A. E. Motter, "Multifaceted Dynamics of Janus Oscillator Networks," *Phys. Rev. X*, 2019.

[5] G. Filatrella, A. H. Nielsen, and N. F. Pedersen, "Analysis of a power grid using a Kuramoto-like model," *Eur. Phys. J. B*, 2008.

[6] T. Nishikawa and A. E. Motter, "Comparative analysis of existing models for power-grid synchronization," *New J. Phys.*, 2015.

[7] B. Schäfer, D. Witthaut, M. Timme, and V. Latora, "Dynamically induced cascading failures in power grids," *Nat. Commun.*, 2018.

[8] P. J. Menck, J. Heitzig, J. Kurths, and H. J. Schellnhuber, "How dead ends undermine power grid stability," *Nat. Commun.*, vol. 5, 2014.

[9] H. Kim, S. H. Lee, and P. Holme, "Building blocks of the basin stability of power grids," *Phys. Rev. E*, 2016.

[10] C. Mitra, A. Choudhary, S. Sinha, J. Kurths, and R. V. Donner, "Multiple-node basin stability in complex dynamical networks," *Phys. Rev. E*, 2017.

[11] Z. Liu, X. He, Z. Ding, and Z. Zhang, "A Basin Stability Based Metric for Ranking the Transient Stability of Generators," *IEEE Trans. Ind. Informatics*, 2019.

[12] J. Machowski, J. W. Bialek, and J. R. Bumby, *Power System Dynamics: Stability and Control*. John Wiley & Sons, 2008.